

Electronic Supplementary Information

A Zr-cluster based thermostable, self-healing and adaptive metallogel with chromogenic properties responds to multiple stimuli with reversible radical interaction

*Ya-Jun Zhang, Feng-Juan Shen, Ya-Juan Li, Xue-Lei Pang, Cong Zhang, Jujie Ren, and Xu-Dong Yu**

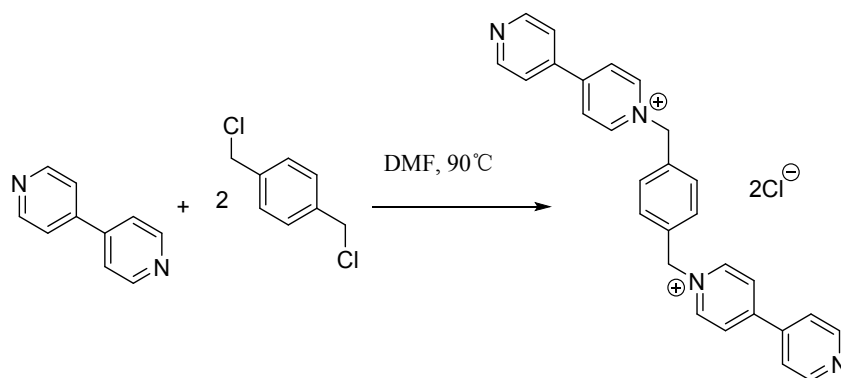
*College of Science, Hebei University of Science and Technology, Yuhua Road 70,
Shijiazhuang 050080, China*

E-mail: chemyxd@163.com (X. Yu)

Section 1. Materials and instruments

All chemicals were purchased from commercial sources and were of GR/AR grade and used without further treatment. The X-ray Photoelectron Spectroscopy analysis was performed using Thermo Scientific Escalab 250 Xi. Electron spin resonance (ESR) signals were recorded on a MiniScope MS5000 EPR spectrometer (Magnettech). Infrared spectra were recorded on an IRPRESTIGE-21 spectrometer (Shimadzu). Morphologies of the xerogels were measured by using FE-SEM S-4800 instruments (Hitachi). TEM images were recorded by JEM-2100 (JEOL). ^1H NMR spectra were recorded on a Bruker Advance DRX 400 spectrometer operating at 500 MHz. The chemical shifts were measured relative to TMS (0.00 ppm) for DMSO- D_6 as indicated. UV-vis absorption spectra for both solutions and gels were obtained on a UV-vis 2550 spectroscope (Shimadzu) with a scanning range of 200–800 nm. The rheological behaviour and the strain-stress properties of gels were measured using a controlled-stress rheometer (Malvern Bohlin Gemini HR Nano), and a vertebral plate geometry of 40 mm was used for the tests on freshly prepared gel samples. The XRD data were analyzed with a Bruker AXS D8 instrument (Cu target; $\lambda = 0.1542$ nm, Germany). Fluorescence measurements in both solution and gel state were performed at 298 K on an Edinburgh Instruments FLS-920 spectrometer by using a Xe lamp as the excitation source. Cyclic voltammogram and Nyquist plots were obtained by using CHI600D Electrochemical workstation. HRMS was performed on Solarix-70FT-MS instrument.

Section 2. Schemes and Figures



Scheme S1 The synthesis process of L·2Cl⁻.

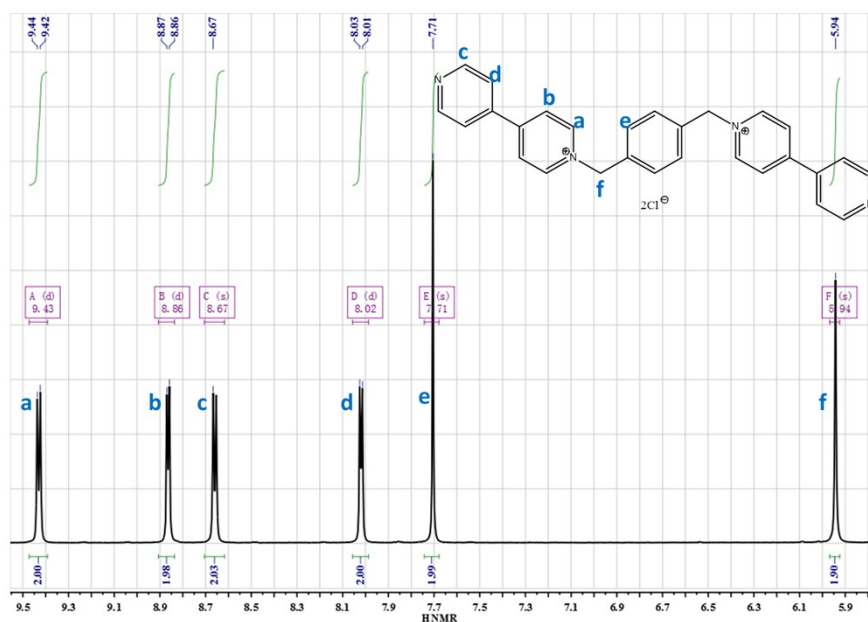


Figure S1 ^1H NMR (400 MHz, DMSO-d_6) spectra of $\text{L}\cdot 2\text{Cl}^-$.

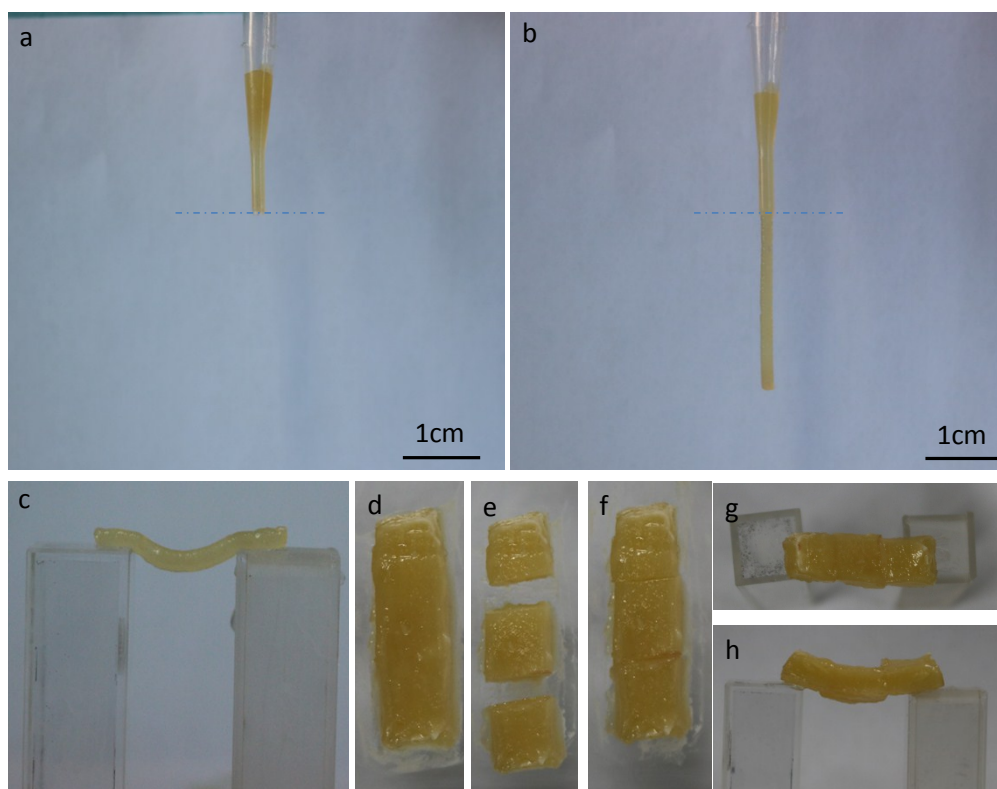


Figure S2 (a-c) Photos showing the injectable and self-supporting characteristics of Zr-gels. (a) gel in dropper; (b) gel was extruded; (c) gel was supported by fluorescence cell. (d-h) Photos demonstrating the self-supporting and self-healing properties of Zr-gel. (d) gel block; (e) gel was cut to pieces; (f) healed gel after minutes; (g) and (h) healed gel was supported by fluorescence cell.

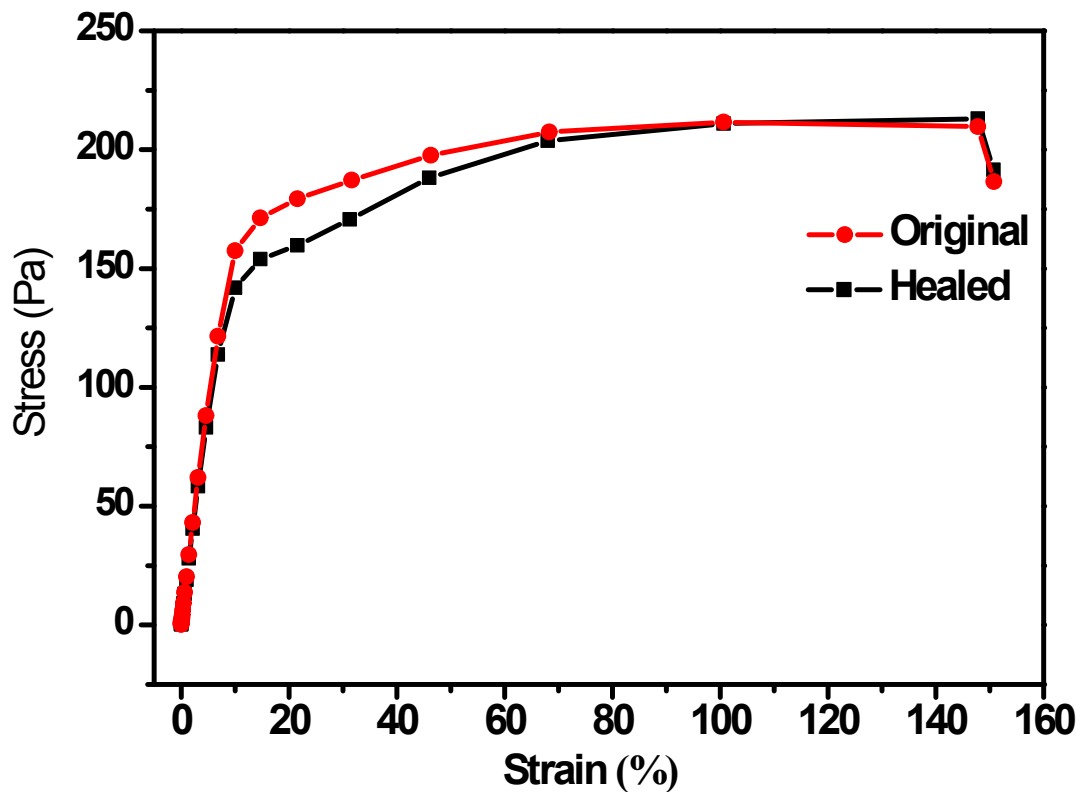


Figure S3 Stress-strain curve for representative original and healed samples of Zr-gel.¹ The gel sample was cut into completely separate pieces using a razor blade and the cut faces were gently brought together at some temperature for 2 minutes. It revealed that the values of stress recovered to 88%-98% of the original gel (in the range of strain from 14% to 70%). Note: it was a stress test rather than tensile test.

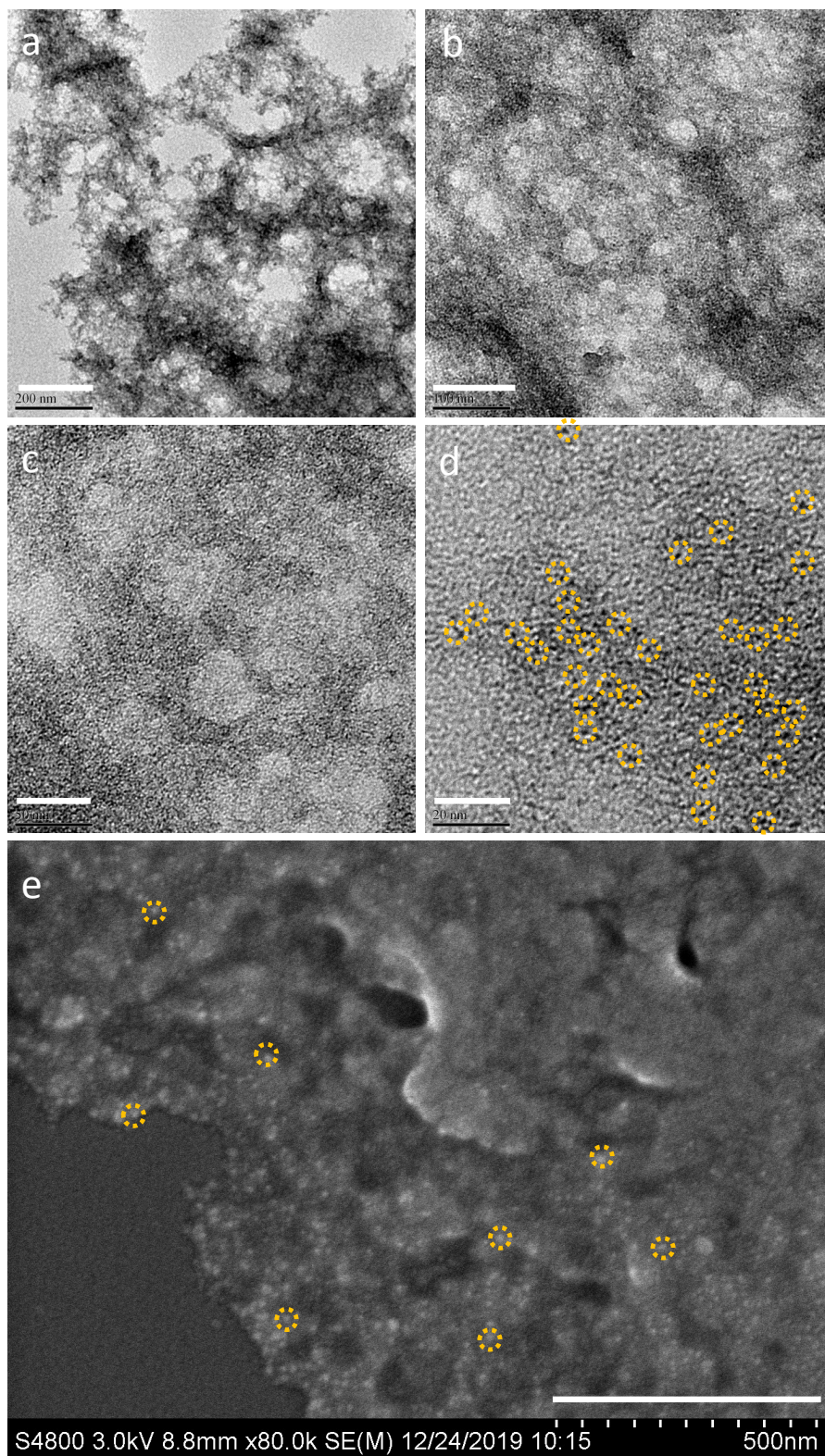


Figure S4 (a) TEM images of Zr-xerogel; (b) magnification picture of (a); (c) magnification picture of (b); (d) magnification picture of (d); (e) SEM image of Zr-gel, uniformly distributing bright dots representing the aggregates of Zr clusters. Note: some of Zr clusters are highlighted by yellow dotted circles (diameters range from 1 nm to 3 nm). Scale bar: (a) 200 nm; (b) 100 nm; (c) 50 nm; (d) 20 nm; (e) 500 nm.

Table S1 The semiquantitative analysis of the elements in the metallogel from energy dispersive X-ray spectroscopy (EDXS). Note: K and L represent corresponding electronic shell.

Element	Weight%	Atomic%
C K	33.64	43
N K	10.07	11.75
O K	43.59	41.90
Cl K	4.65	2.02
Zr L	8.05	1.33
Totals	100.00	

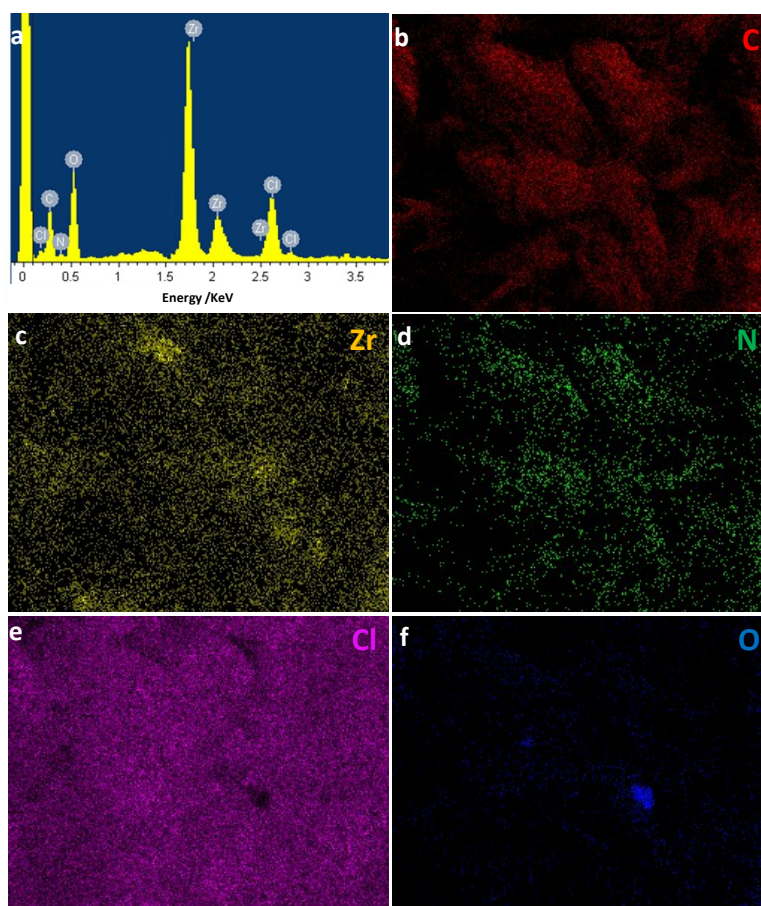


Figure S5 (a) The EDX spectrum of Zr-xerogel showing the intensity of corresponding elements; (b)-(f) The corresponding EDX mapping of elements C (b), Zr (c) N (d), Cl (e) and O (f) in Zr-xerogel.

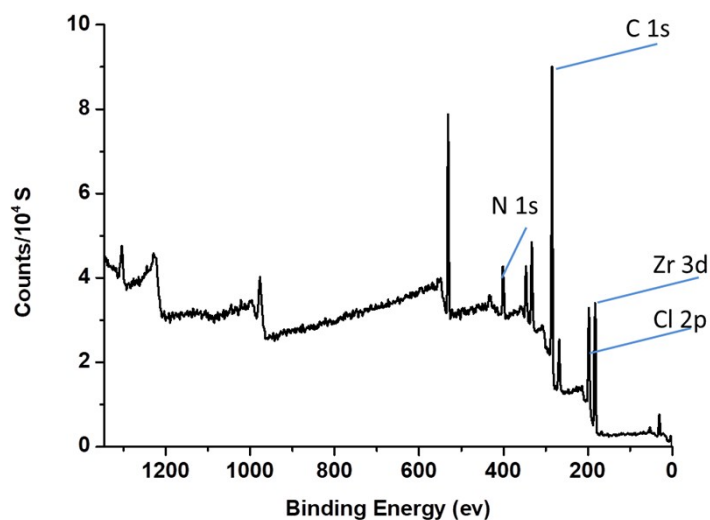


Figure S6 The XPS surface analysis of the Zr-xerogel.

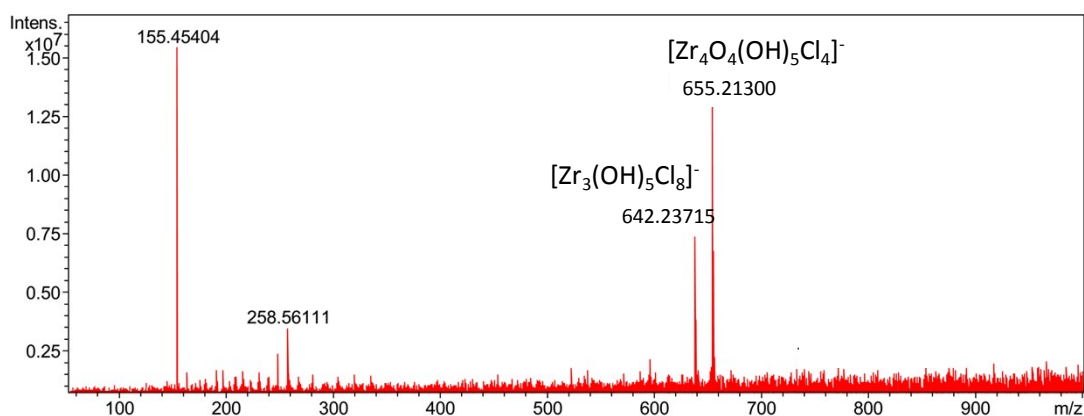


Figure S7 HRMS spectra of Zr-Xerogel, showing the existence of polynuclear zirconium species such as [Zr₃(OH)₅Cl₈]⁻ and [Zr₄O₄(OH)₅Cl₄]⁻.

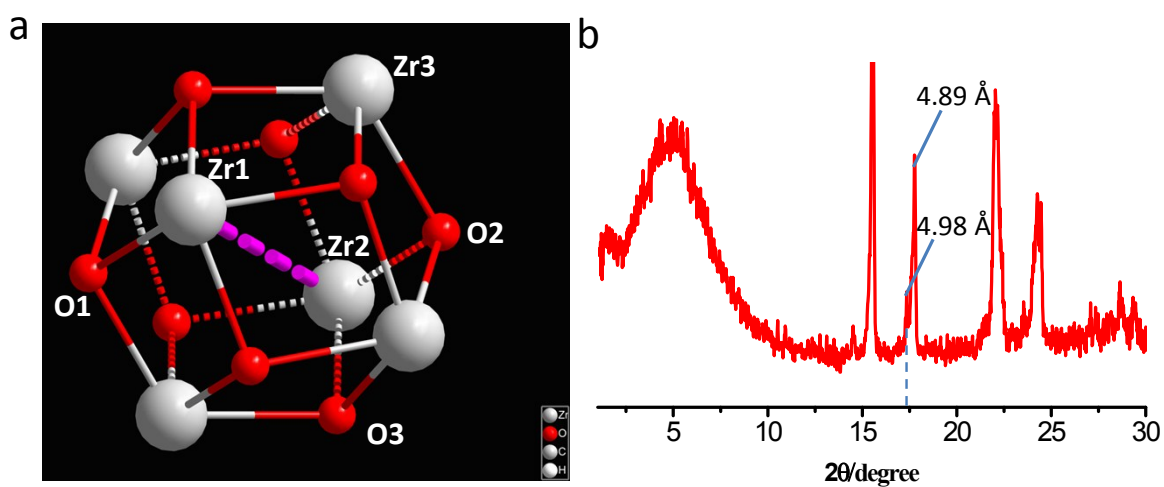


Figure S8 (a) The structure of Zr₆ cluster in MOF-812 and the distance of diagonal zirconium (Zr1-Zr2), O1-O2 were measured by diamond software for 4.98 Å, 4.89 Å separately as seen from literature,² which was obtained by by Bragg's law; (b) X-ray powder diffraction (XRD)

of the Zr-xerogel, and two peaks coinciding with the two distances on $2\theta = 17.74$ and 18.07 by Bragg's law.

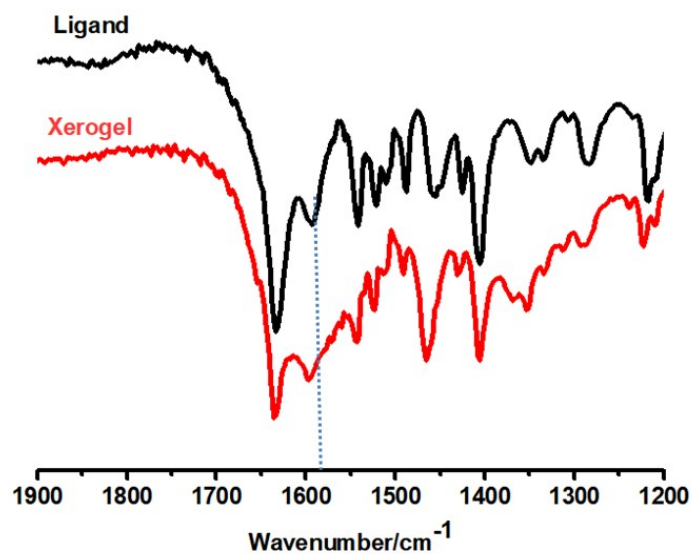


Figure S9 Fourier transform infrared (FTIR) spectra of the xerogel (Red line) and Ligand (Dark line).

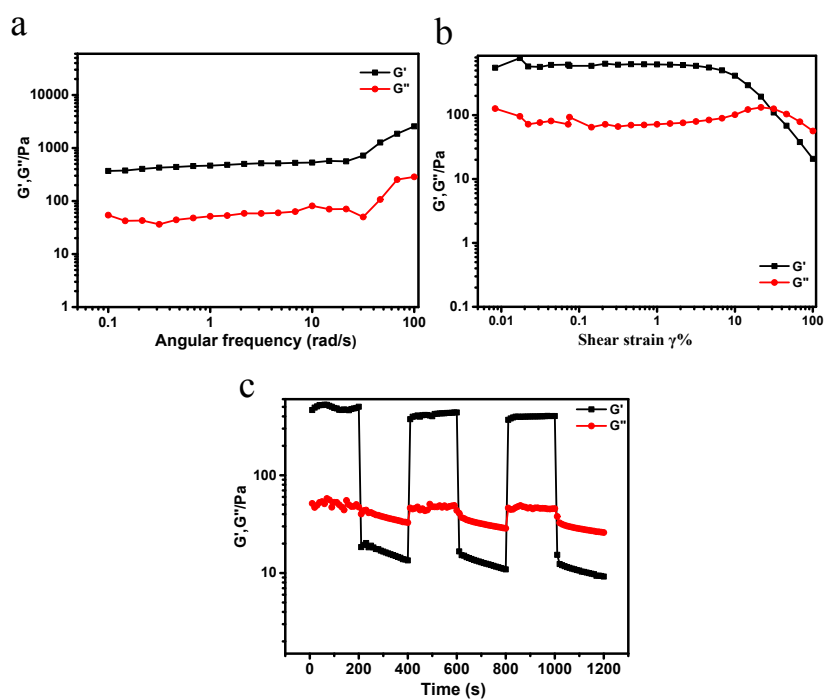


Figure S10 Static oscillation frequency sweeps (a), dynamic strain sweep (b) measurements and recovery experiments (c) of the Zr-gels.

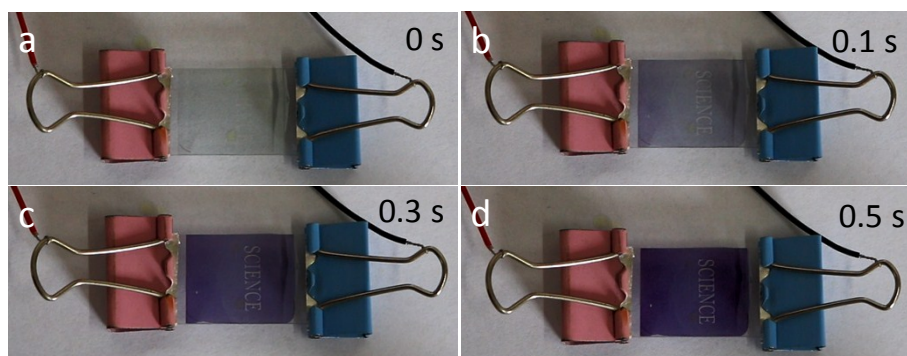


Figure S11 The three-layered color-changing device was constructed of “ITO coated glass/Zr-gel/ITO” coated glass which etched word ‘SCIENCE’. The degree of coloration for Zr-gel within 0 s (a), 0.1 s (b), 0.3 s (c), 0.5 s (d) after power on, showing the etched word “SCIENCE”. When air is further dipped into the gel, the color and word disappear again. Such process could be repeated for many circles without fatigue.

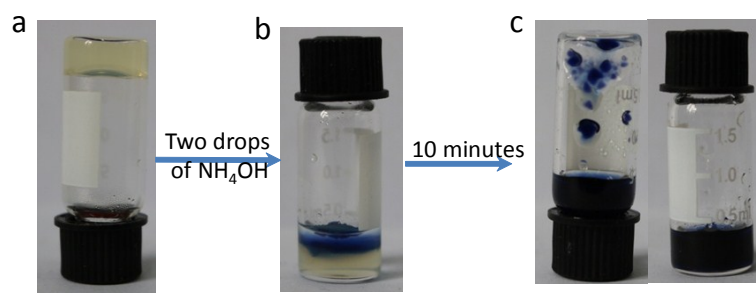


Figure S12 Illustration for gel-sol transformation of Zr-gel by the addition of two drops of NH_4OH , the gel collapse in ten minutes and the color changes. a) the original Zr-gel; b) the changes of Zr-gel with addition of NH_4OH ; c) the changes of Zr-gel with NH_4OH for 10 minutes.

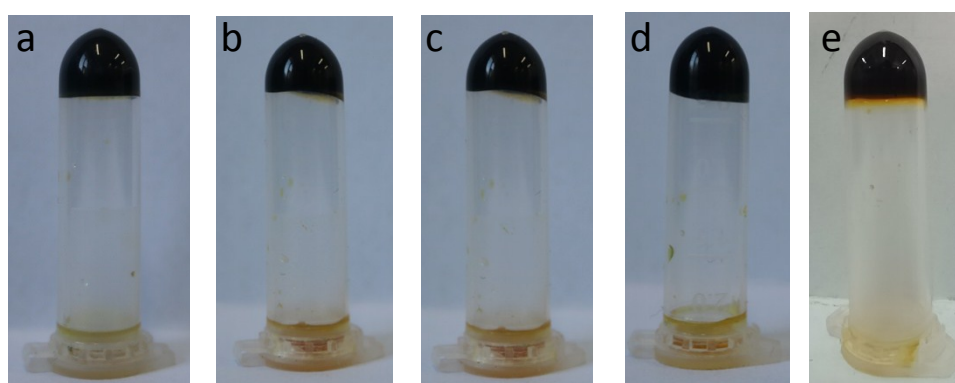


Figure S13 The images of Zr-gels triggered by three drops of different kinds of aliphatic amines. (a) Ethylene diammine, (b) cis-1,2-cyclohexane diamine, (c) triethylamine, (d) propargylamine, (e) diisopropylamine.

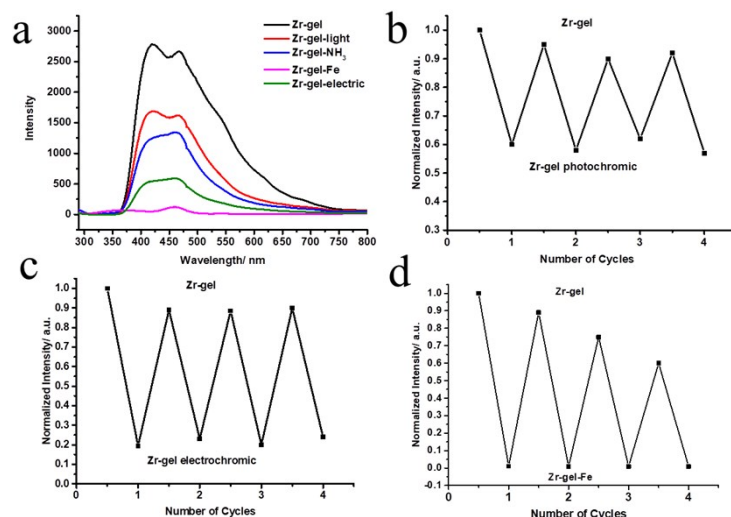


Figure S14 (a) Fluorescence spectra of Zr-gel, Zr-gel-light, Zr-gel-NH₃, Zr-gel-electric, Zr-gel-Fe; (b) Cycle experiments of fatigue resistance of Zr-gel on the reversible fluorescent regulation by the light, electricity and Fe ($\lambda_{ex}=270$ nm).

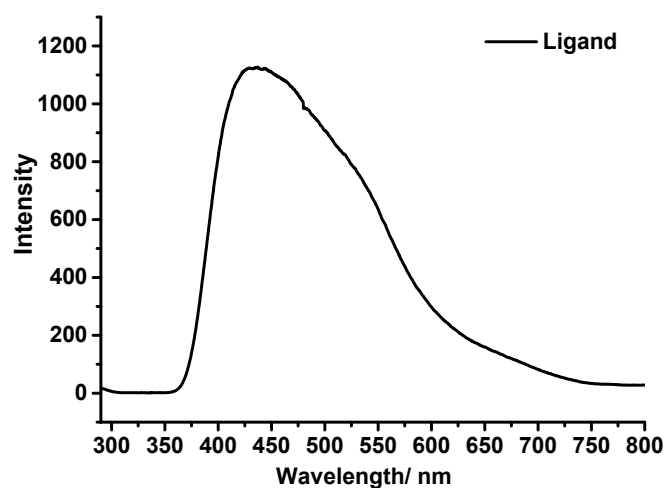


Figure S15 Fluorescence spectra of Ligand in DMF ($\lambda_{ex}=270$ nm).

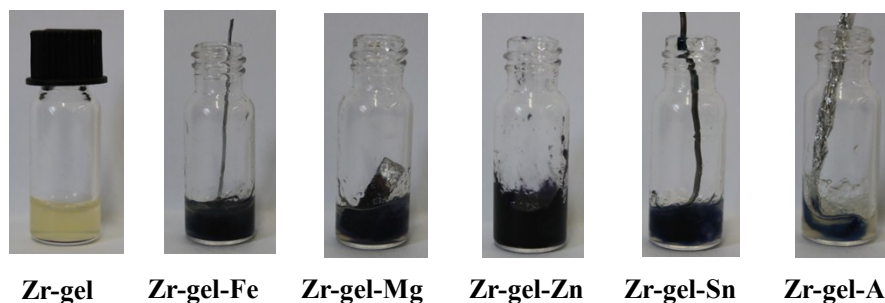


Figure S16 Images of Zr-gel, Zr-gel-Fe, Zr-gel-Zn, Zr-gel-Sn and Zr-gel-Al.

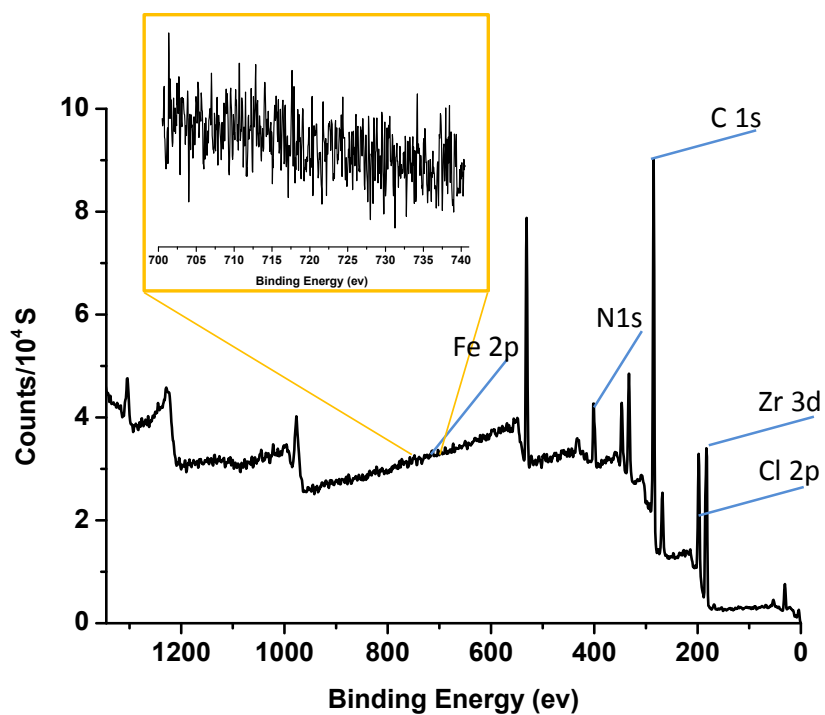


Figure S17 X-ray photoelectron spectroscopy (XPS) measurements of Zr-gel-Fe xerogel.

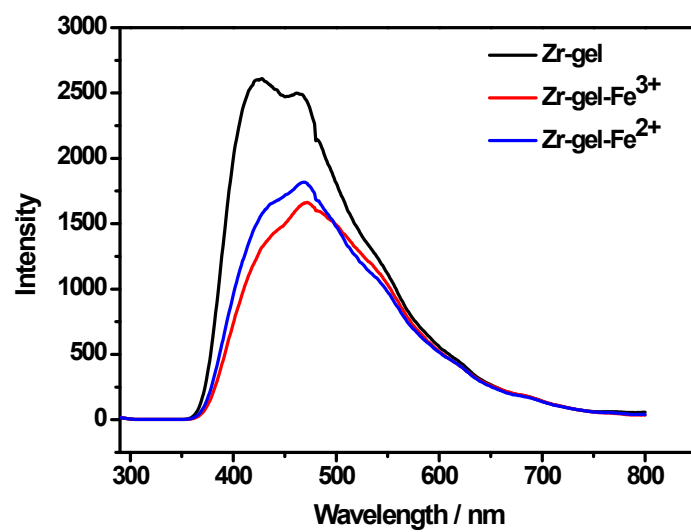


Figure S18 Fluorescence spectra of Zr-gel and Zr-gels upon the addition of 200 μL Fe³⁺ and Fe²⁺solutions (10⁻⁴ M).

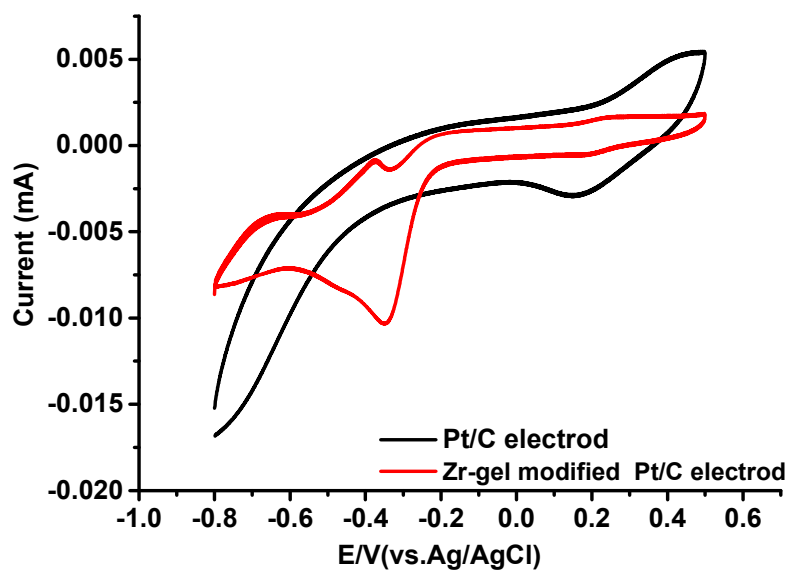


Figure S19 Cyclic voltammogram obtained using Pt/C electrode (black line) in 0.1 M PBS solution (pH=7.4) and Zr-gel modified Pt/C electrode (red line) as the working electrode and the potential scan rate was 0.1 V/ s.

References

1. (a) Y. Gao, Q. Luo, S. Qiao, L. Wang, Z. Dong, J. Xu, J. Liu, *Angew. Chem. Int. Ed.* **2014**, 53, 9343-9346; (b) B. Michal, C. A. Jaye, E. J. Spencer, S. J. Rowan, *ACS Macro Lett.* **2013**, 2, 694-699; (c) D. Taylor, M. Panhuis, *Adv. Mater.* **2016**, 28, 9060-9093; (d) A. Ciferri, *Polym. Chem.* **2013**, 4, 4980-4986.
2. H. Furukawa, F. Gándara, Y. Zhang, J. Jiang, W. L. Queen, M. R. Hudson, and Omar M. Yaghi, *J. Am. Chem. Soc.* **2014**, 136, 4369–4381.